AN IN-SILICO APPROACH TO DESIGN AND DISCOVER EPICATECHIN-BASED DUAL INHIBITORS OF A AMYLASE AND A GLUCOSIDASE

Simran Kumari Srivastava[1], Komal Manwani[2], Sonam Singh Parmar[3], Dr. Prashant Kumar Katiyar[4]

[1] Research Scholar, Kanpur Institute of Technology and Pharmacy, Kanpur, UP, India

[2] Assistant Professor, Kanpur Institute of Technology and Pharmacy, Kanpur, UP, India

[3]Assistant Professor, Kanpur Institute of Technology and Pharmacy, Kanpur, UP, India

[4] Director, Kanpur Institute of Technology and Pharmacy, Kanpur, UP, India

Corresponding Author – Simran Kumari Srivastava

simran161296@gmail.com[1], komal.manwani@kit.ac.in[2], sonam.parmar@kit.ac.in[3] , prashant.katiyar@kit.ac.in[4]

ABSTRACT

Diabetes is a prevalent metabolic disorder characterized by elevated blood glucose levels due to impaired glucose metabolism. Current therapeutic approaches target enzymes involved in carbohydrate digestion and absorption, such as α-amylase and α-glucosidase, to control postprandial hyperglycemia. In this study, we designed and evaluated 100 zinc-based derivatives of epicatechin as potential inhibitors of these enzymes. Epicatechin, a natural flavonoid found in various plants, has shown promising inhibitory activity against α-amylase and α-glucosidase. By incorporating zinc into epicatechin derivatives, we aimed to enhance their binding affinity and inhibitory potency. Docking studies were conducted to assess the binding affinity of the designed compounds with α-amylase and α-glucosidase. Several derivatives demonstrated strong binding affinity to the active sites of both enzymes, outperforming the reference compound Acarbose. Further analysis revealed extensive hydrogen bonding and miscellaneous interactions of the designed compounds with key residues in α-amylase and α-glucosidase. These interactions suggest the potential of the zinc-based derivatives to disrupt the enzymes' active sites and inhibit their catalytic activities effectively. ADME analysis indicated favorable pharmacokinetic properties for the compounds, such as molecular weight and hydrogen bond donors and acceptors, crucial for drug-protein interactions and solubility. Additionally, computational toxicity analysis showed a generally low toxicity profile for the zinc-based derivatives. In conclusion, this study presents the design and evaluation of 100 zinc-based derivatives of epicatechin as potential inhibitors of α-amylase

and α-glucosidase. The computational analysis reveals compounds with strong binding affinity and inhibitory potential, providing a basis for further experimental investigations. Developing novel inhibitors targeting these enzymes could offer new therapeutic strategies for managing abnormal carbohydrate metabolism in diabetes.

KEYWORDS: Diabetes, Epicatechin, α-amylase, α-glucosidase, ADME, Toxicity

INTRODUCTION

Diabetes is a chronic metabolic disorder characterized by elevated levels of glucose in the bloodstream. Normally, food is broken down into glucose in the stomach and serves as an energy source for the body [1]. The pancreas plays a crucial role in this process, housing three types of cells: α, beta, and delta cells. Among them, beta cells are responsible for producing insulin, a hormone that regulates blood glucose levels and facilitates the transfer of glucose to various parts of the body, including muscles, fats, and the liver [2-3]. However, in individuals with diabetes, this vital function of glucose transfer encounters resistance due to two primary factors. There are two main reasons for the increase in blood glucose levels in individuals with diabetes:

1. Insufficient insulin production by pancreatic beta cells: In this case, the beta cells in the pancreas fail to produce an adequate amount of insulin [4]. Without enough insulin, glucose cannot be effectively transferred from the bloodstream into cells to be used as energy. This leads to elevated blood glucose levels [5].
2. Insulin resistance: Insulin resistance occurs when cells in the body do not respond to insulin normally. In other words, even if sufficient insulin is produced, the cells fail to effectively utilize it to allow glucose to enter and be stored for energy [6]. As a result, glucose accumulates in the bloodstream, causing high blood sugar levels [7].

There are three main types of diabetes:

1. **Type 1 diabetes (T1D) or Juvenile diabetes or Insulin-dependent diabetes**: T1D can affect individuals of any age, including both adults and children [8]. It occurs when the pancreas stops producing insulin due to the destruction or inactivity of pancreatic beta cells. People with T1D rely on daily insulin injections to maintain normal blood glucose levels [9]. The exact causes of T1D are not fully understood, but it is believed that a combination of genetic and environmental factors contributes to its development.

2. **Type 2 diabetes (T2D) or Non-insulin dependent diabetes mellitus (NIDDM)**: This is the most common form of diabetes and is typically diagnosed in adulthood. However, due to rising obesity rates and sedentary lifestyles, T2D is increasingly being diagnosed in teenagers and young adults as well. In T2D, fat, muscle, and liver cells do not respond properly to insulin, leading to insulin resistance. Consequently, blood sugar cannot enter these cells for energy storage, resulting in its accumulation in the bloodstream. Insulin resistance is a gradual process that develops over time [10].

3. **Gestational diabetes**: Gestational diabetes is a type of diabetes that is first diagnosed during pregnancy. Approximately eight out of 100 pregnant women in the United States develop gestational diabetes [11]. Weight gain and hormonal changes during pregnancy can impair insulin function, leading to high blood sugar levels. Usually, this form of diabetes disappears after pregnancy [12]. However, women who have had gestational diabetes have a 40-60% chance of developing T2D within 5 to 10 years [13].

Epicatechin, a natural flavonoid found in green tea, possesses powerful antioxidant properties and is associated with numerous therapeutic benefits. It has been shown to have a positive impact on various diseases, particularly diabetes and cancer. In the case of diabetes, epicatechin consumption has demonstrated the ability to lower blood glucose levels and help maintain them within the standard range [14]. Although the exact mechanism of action of epicatechin in diabetes treatment is still being investigated, its potential as a promising candidate cannot be ignored. Emerging evidence suggests that epicatechin, as a Flavon-3-ol compound, plays a role in improving insulin sensitivity and may have a significant impact on the progression of Type 2 diabetes. By incorporating epicatechin-rich diets into their routine, individuals with insulin resistance and glucose intolerance, such as those with obesity and Type 2 diabetes, may experience normalized insulin sensitivity and glucose regulation [15]. Epicatechin compounds also exhibit inhibitory effects on various biological events, including inflammation, oxidative stress, and endoplasmic reticulum stress. Furthermore, they regulate processes within the gastrointestinal tract and pancreas, ultimately influencing glucose homeostasis [16]. While the precise mechanisms by which epicatechin influences diabetes treatment are yet to be fully elucidated, its antioxidant effects and potential therapeutic actions make it a promising natural compound for managing the disease. Further research is needed to fully understand and harness the benefits of epicatechin in diabetes and other ailments [17-20].

The objective of this study is to conduct *in silico* analysis of zinc-based epicatechin derivatives for diabetes by targeting α-amylase and α-glucosidase, including molecular docking, ADME prediction, and interaction studies. The specific goals are to investigate epicatechin's binding affinity and interactions with target proteins involved in glucose regulation, predict its absorption, distribution, metabolism, and excretion properties, analyze molecular interactions, evaluate its drug-likeness properties, perform virtual screening for potential targets, validate findings with existing data, and provide insights for future research. This analysis aims to assess the therapeutic potential of epicatechin as an anti-diabetic agent and contribute to the development of novel interventions for diabetes management.

MATERIAL AND METHODS

In this study, in-silico docking, a widely utilized technology for screening molecular libraries, was employed to identify potential compounds with enzymatic inhibition capabilities. The Vina 1.5.6 AutoDock tool was utilized to assess the binding affinity (Kcal/mol) of the compounds, specifically focusing on their interaction with the selected protein targets, namely α-glucosidase (PDB id: 3a4a) and α-amylase (PDB id: 4w93) [21]. The compounds, obtained from the ZINC database, were represented in both 2D and 3D structures using ChemBiodraw ultra and ChemBiodraw 3D programs. Optimization of the compounds' performance and energy minimization was achieved through the implementation of the MM2 method. The resulting compounds were analyzed for their potential as α-amylase and α-glucosidase dual inhibitors, and the interactions and poses of the compounds were visualized using Biovia discovery studio visualizer and Pymol software.

COMPUTATIONAL DETAILS

Virtual Screening of Potential Molecules

In this study, a library of potential chemical compounds was generated by searching the ZINC small molecule database for commercially available substances. Epicatechin was chosen as the representative molecule for this analysis. The ZINC database, accessible at (www.zinc.docking.org), was used to identify structurally similar compounds, resulting in the discovery of approximately 40% of such compounds. These molecules were downloaded in the structural database file (.sdf) format. The Marwin view 18.22 version was employed to open and visualize the downloaded ZINC database (.sdf) file, allowing for further analysis and investigation [22].

Ligand Preparation

To determine the most promising epicatechin derivative with strong binding potential, a comprehensive screening was conducted using a library of these compounds. The 2D structures of the epicatechin derivatives were generated using ChemBioDraw 2D software. Additionally, ChemBioDraw 3D software was employed to convert the ligands into their respective three-dimensional structures. Finally, to facilitate ligand analysis using the Autodock Vina program, the ligands were saved as .PDB files, enabling further investigation of their binding affinities and interactions with target proteins [23-24].

Protein Selection and Preparation

Proteins with the PDB codes 3a4a and 4w93, representing α-glucosidase and α-amylase, respectively, were obtained from the Protein Data Bank (https://www.rcsb.org/). These proteins, known for their roles in glucose metabolism, were downloaded and prepared using the AutoDock Vina program. The program facilitated the separation of the ligand and protein components for further analysis. The main objective of utilizing AutoDock Vina in this study is to identify potential compounds with a high binding affinity for α-glucosidase (3a4a) and α-amylase (4w93). By investigating the binding interactions between the ligands of interest and these enzymes, the study aims to discover promising compounds that could potentially modulate glucose metabolism and be developed as therapeutic agents for metabolic disorders such as diabetes [25].

Validation of Protein for Docking

The repeatability and validity of the approach were assessed using the root mean square deviation (RMSD) to compare redocked binding sites with ligands' atomic and crystallographic conformations. The RMSD served as a quantitative measure, evaluating the accuracy and precision of the methodology. Repeatability was determined by calculating the RMSD across multiple redocking iterations, assessing consistency. Validity was established by comparing the redocked binding sites with crystallographic conformations, indicating accuracy. The lower the RMSD value, the higher the repeatability and validity, suggesting consistent and accurate prediction of binding site conformations. The use of RMSD provided a robust evaluation of the approach's performance [26].

Molecular Docking study

Molecular docking was conducted to explore the potential binding patterns of the designed molecules SS1-100 with the active sites of the target enzymes α-amylase (PDB ID: 4w93) and α-glucosidase (3a4a), using AutoDock Vina 1.5.6. The protein was validated by extracting the ligand from the protein structure, followed by preparation for the docking study. This involved adding polar hydrogen, identifying the root, and converting the structure to a pdbqt extension file. The protein was further prepared by removing water molecules, fixing missing atoms, adding polar hydrogen, and assigning Kollman charges [27]. A grid box was generated around the ligand, with the following coordinates and sizes for -amylase (PDB ID: 4w93) and α-glucosidase (3a4a), respectively:

center_x = -9.983

center_y = 5.647

center_z = -22.996

size_x = 54

size_y = 42

size_z = 40.

center_x = 21.798

center_y = -7.787

center_z = 24.341

size_x = 30

size_y = 24

size_z = 22

The AutoDock Tool Vina was executed through the command prompt, using the command "program files\the scripps research institute\vina\vina.exe -config conf.txt -log log.txt." The docking results, including binding affinities (Kcal/mol), for both the designed molecules and the standard acarbose, were recorded and presented in a table [28].

ADME Analysis to find the lead molecules

The screening and evaluation of seven hit compounds were conducted using the SwissADME server, which is a computational tool for assessing molecular properties. The compounds were inputted into the SwissADME program using a molecular sketcher based on ChemAxon's Marvin. This allowed for the importation or manual drawing of 2D chemical structures, as well as the utilization of SMILES notation. The BIOLED-egg approach within SwissADME was employed to analyze various physiochemical characteristics, including interactions with p-glycoprotein, permeability across the blood-brain barrier according to Lipinski's rule of 5, and gastrointestinal absorption. By employing this computational approach, lead compounds with desirable properties for targeted opioid agonists were identified based on lead-likeness criteria. Furthermore, PKCSM (Preclinical Knowledge-Based Consensus Model) was utilized to evaluate the toxicity of the identified lead compounds [29-30]. PKCSM employs a knowledge-based consensus model that integrates multiple toxicity prediction models and databases to provide a comprehensive assessment of potential toxicity risks. By leveraging PKCSM, the research aimed to ensure that the selected lead molecules not only exhibited favorable pharmacological properties but also demonstrated low toxicity profiles, thereby increasing their potential as safe and effective drug candidates for targeted opioid agonists. This integrated approach combining SwissADME and PKCSM enabled a robust evaluation of the lead compounds' suitability for further development [31-33].

RESULT & DISCUSSION

The provided **table 1** presents the docking scores of various compounds compared to acarbose in terms of their binding affinity to α-amylase and α-glucosidase. Docking scores, obtained through computational simulations, provide valuable insights into the potential interactions between ligands (compounds) and target proteins. In this case, the target proteins, α-amylase and α-glucosidase, play crucial roles in carbohydrate metabolism, and the compounds listed in the table are being evaluated for their potential as inhibitors of these enzymes. Upon analyzing the data, it becomes evident that several compounds exhibit notable binding affinity when compared to acarbose, which serves as a reference inhibitor.

Table 1: Docking score of all the designed 100 compounds along with Ligands and standard

Sr No.	**Compound code**	**Structure**	**α-amylase docking score(kcal/mol)**	**α - glucosidase docking score(**

				kcal/mol)
1.	SS-1	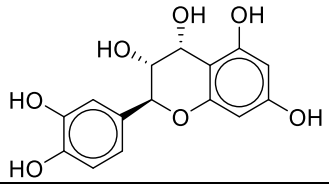	-8.4	-8.2
2.	SS-2	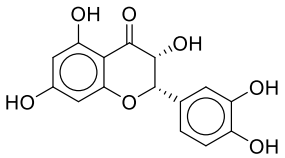	-8.8	-8.5
3.	SS-3	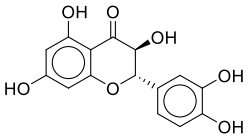	-8.3	-8.6
4.	SS-4	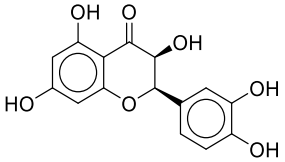	-7.7	-8.3
5.	SS-5	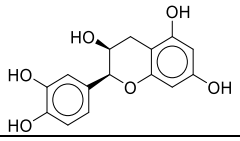	-8.2	-8.4
6.	SS-6	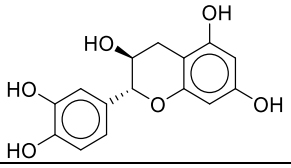	-7.3	-8.5
7.	SS-7	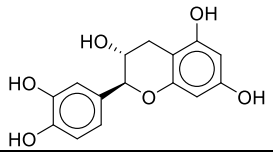	-8.4	-8.6
8.	SS-8	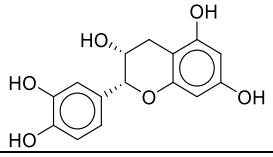	-7.2	-9.0
9.	SS-9	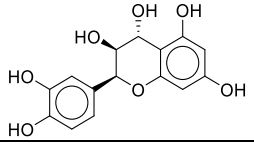	-8.2	-8.2
10.	SS-10	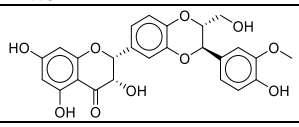	-8.5	-10.0

11.	SS-11	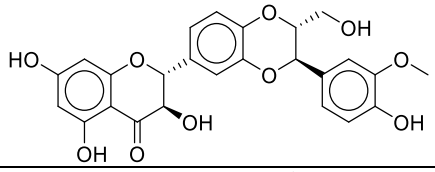	-9.0	-10.1
12.	SS-12	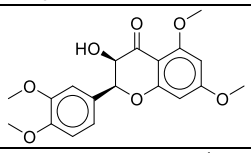	-8.2	-8.2
13.	SS-13	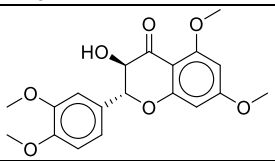	-7.4	-8.1
14.	SS-14	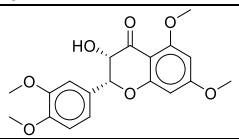	-7.7	-8.0
15.	SS-15	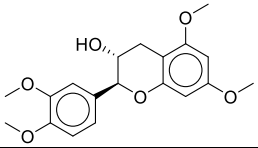	-7.6	-8.1
16.	SS-16	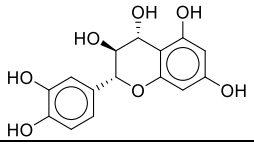	-7.4	8.0
17.	SS-17	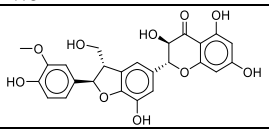	-9.0	-10.1
18.	SS-18	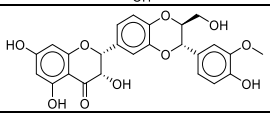	-8.6	-10.3
19.	SS-19	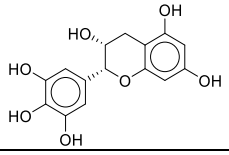	-7.7	-8.6
20.	SS-20	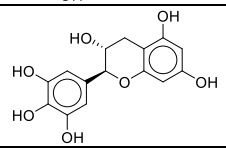	-8.5	-8.2
21.	SS-21	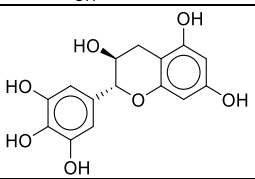	-7.3	-8.7
22.	SS-22	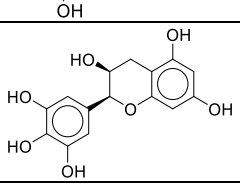	-8.2	-8.8

23.	SS-23	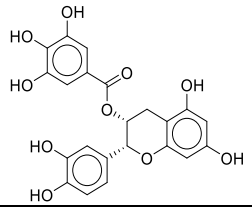	-8.7	-10.2
24.	SS-24	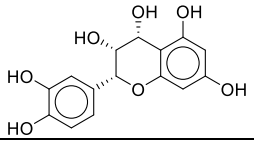	-7.5	-8.9
25.	SS-25	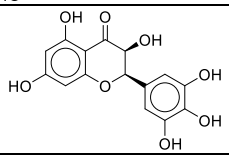	-7.6	-8.3
26.	SS-26	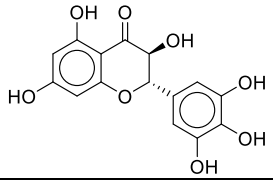	-8.9	-8.8
27.	SS-27	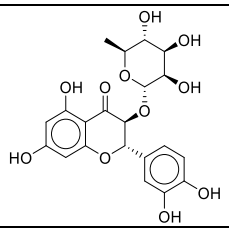	-9.1	-10.7
28.	SS-28	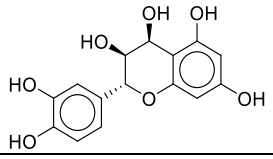	-7.4	-9.0
29.	SS-29	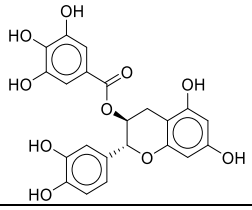	-9.1	-9.5
30.	SS-30	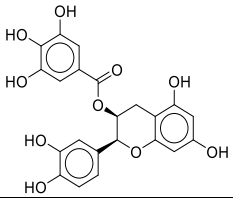	-11.0	-11.3
31.	SS-31	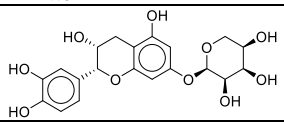	-8.6	-10.0
32.	SS-32	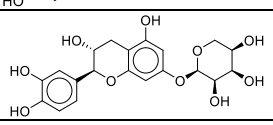	-9.0	-9.9
33.	SS-33	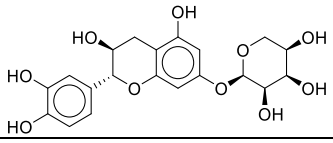	-8.6	-9.7

34.	SS-34	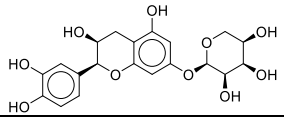	-9.9	-10.1
35.	SS-35	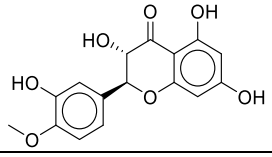	-8.1	-9.1
36.	SS-36	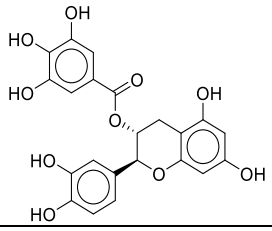	-11.2	-11.3
37.	SS-37	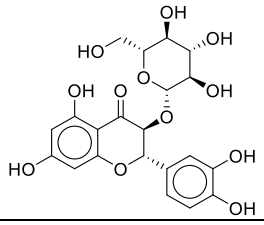	-8.0	-8.9
38.	SS-38	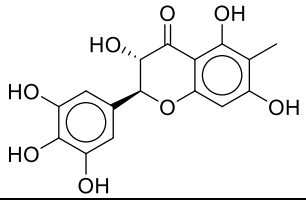	-8.7	-8.8
39.	SS-39	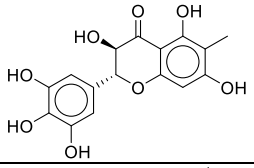	-7.4	-8.5
40.	SS-40	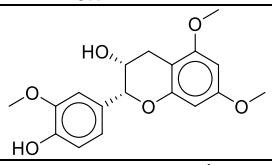	-7.7	7.9
41.	SS-41	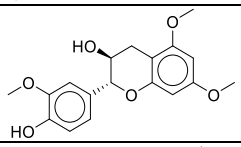	-7.0	8.2
42.	SS-42	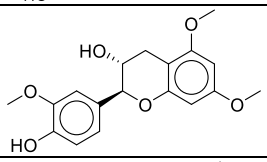	-8.4	-7.9
43.	SS-43	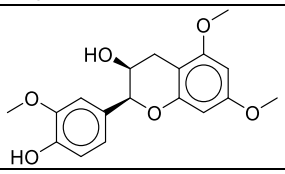	-8.6	-8.0
44.	SS-44	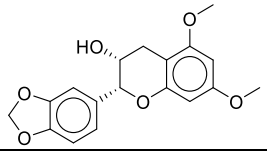	-8.6	-8.6

45.	SS-45	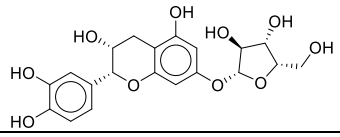	-8.9	-9.5
46.	SS-46	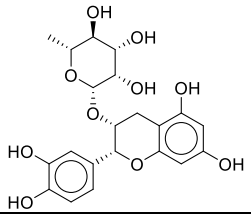	-8.6	-9.1
47.	SS-47	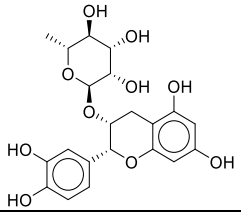	-8.7	-9.7
48.	SS-48	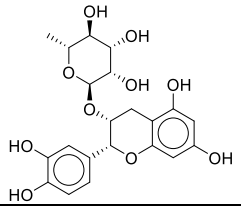	-8.3	-9.5
49.	SS-49	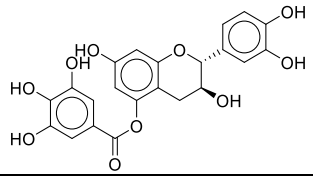	-9.2	-10.5
50.	SS-50	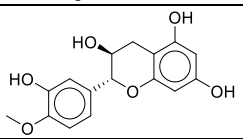	-7.4	-8.0
51.	SS-51	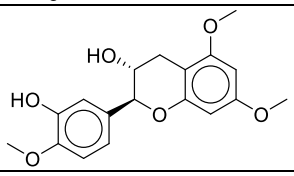	-7.7	-8.4
52.	SS-52	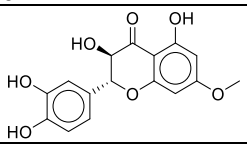	-7.5	-8.0
53.	SS-53	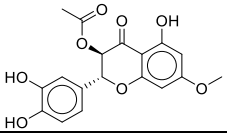	-8.1	-8.6
54.	SS-54	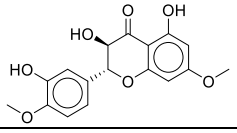	-7.4	-8.3
55.	SS-55	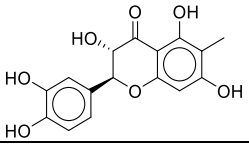	-9.0	8.5

56.	SS-56	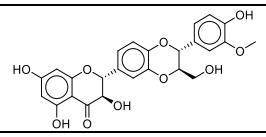	-9.3	-10.0
57.	SS-57	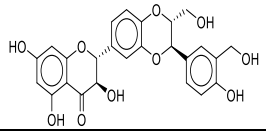	-8.6	-10.0
58.	SS-58	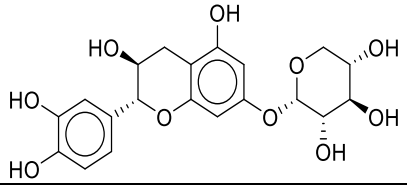	-8.4	-9.9
59.	SS-59	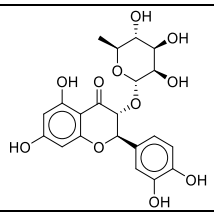	-8.3	-9.5
60.	SS-60	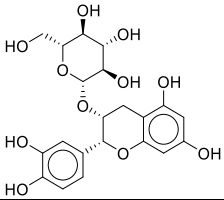	-7.8	-9.2
61.	SS-61	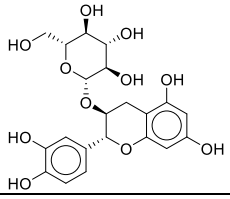	-8.0	-9.5
62.	SS-62	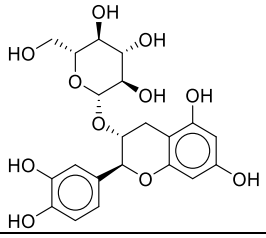	-8.7	-9.0
63.	SS-63	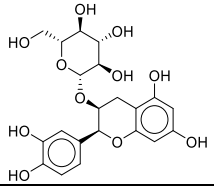	-8.3	-9.0
64.	SS-64	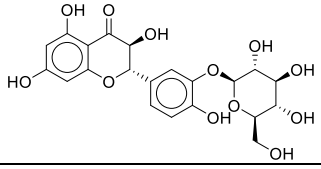	-8.9	-10.0

65.	SS-65	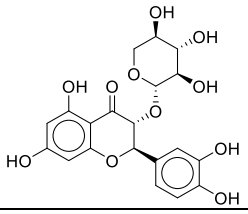	-8.4	-9.5
66.	SS-66	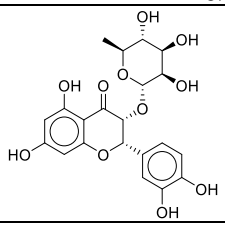	-10.4	-10.4
67.	SS-67	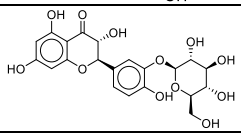	-8.4	-10.0
68.	SS-68	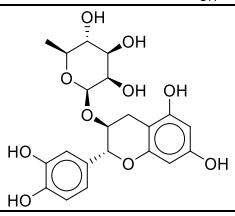	-8.0	-9.3
69.	SS-69	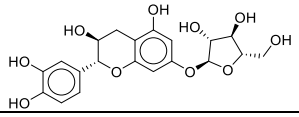	-8.1	-9.2
70.	SS-70	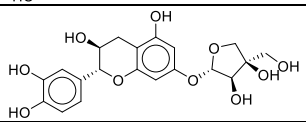	-8.5	-9.4
71.	SS-71	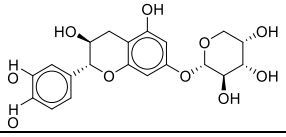	-8.1	-9.7
72.	SS-72	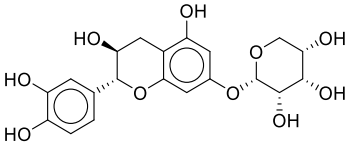	-8.2	-9.9
73.	SS-73	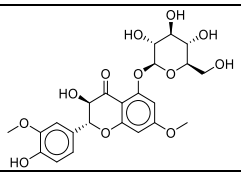	-7.9	-9.0
74.	SS-74	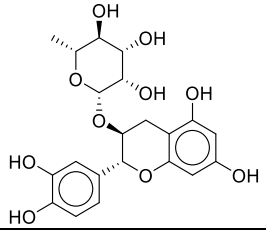	-8.2	-9.4

75.	SS-75	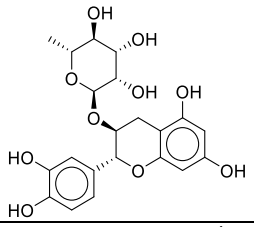	-8.8	-9.4
76.	SS-76	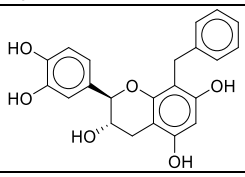	-8.0	-9.2
77.	SS-77	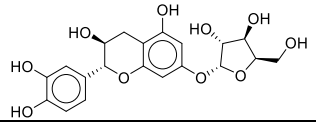	-8.0	-9.3
78.	SS-78	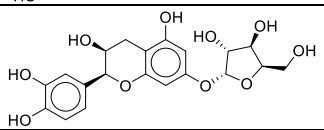	-8.9	-9.4
79.	SS-79	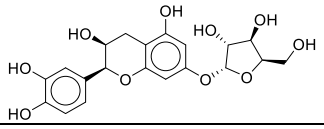	-9.0	-9.6
80.	SS-80	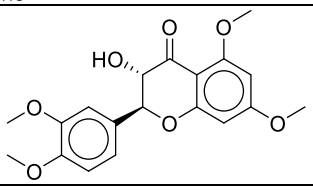	-8.1	-8.0
81.	SS-81	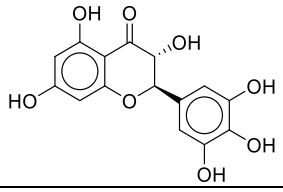	-7.4	-8.5
82.	SS-82	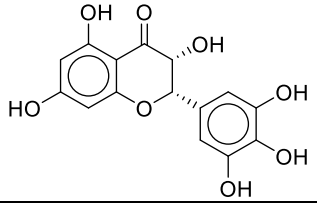	-8.2	-8.3
83.	SS-83	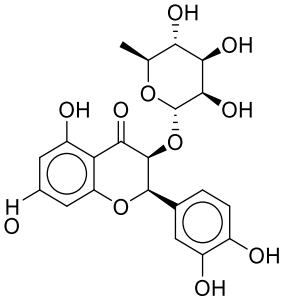	-8.6	-9.5
84.	SS-84	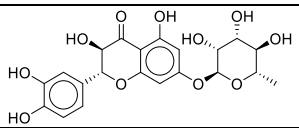	-8.4	-10.6

85.	SS-85	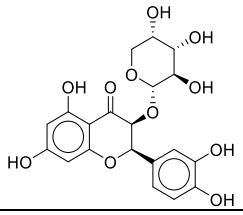	-8.1	-9.6
86.	SS-86	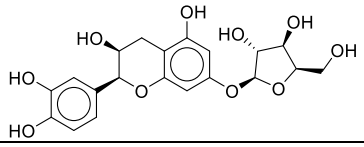	-8.6	-9.9
87.	SS-87	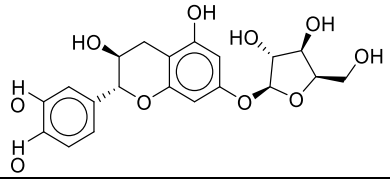	-7.7	-9.0
88.	SS-88	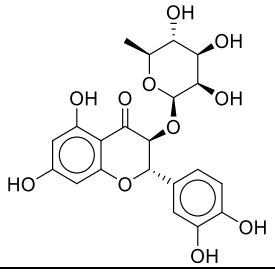	-8.1	-9.3
89.	SS-89	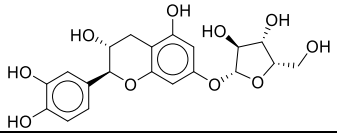	-8.0	-9.6
90.	SS-90	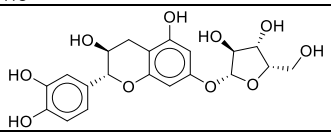	-9.6	-9.9
91.	SS-91	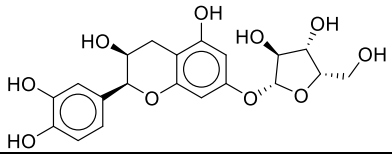	-9.0	-10.2
92.	SS-92	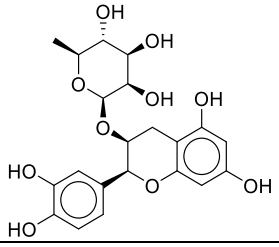	-8.4	-10.3
93.	SS-93	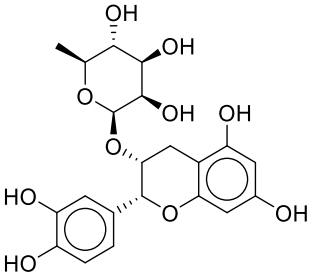	-8.4	-9.6

94.	SS-94	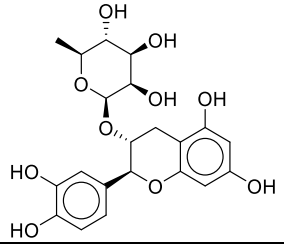	-8.1	-9.3
95.	SS-95	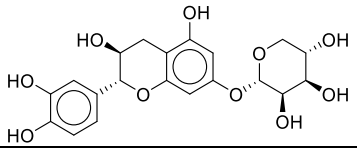	-8.1	-9.8
96.	SS-96	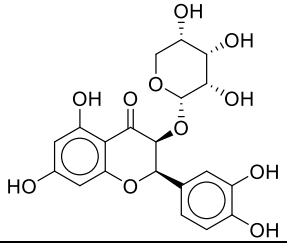	-8.2	-9.8
97.	SS-97	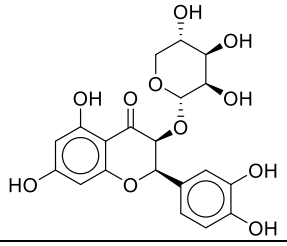	-8.0	-9.4
98.	SS-98	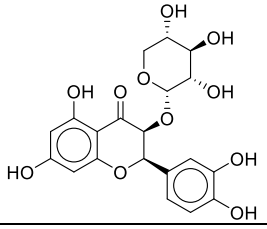	-8.7	-9.4
99.	SS-99	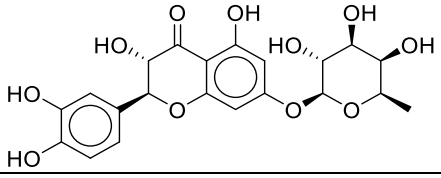	-9.7	-10.1
100.	SS-100	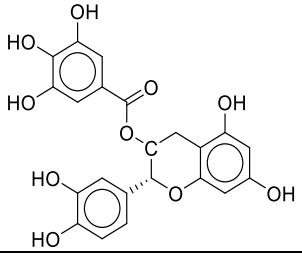	-8.4	-10.0
101	3LN	Ligand for Amylase	-9.3	--
102	GLC	Ligand for Glucosidase	--	-5.5

103	Acarbose	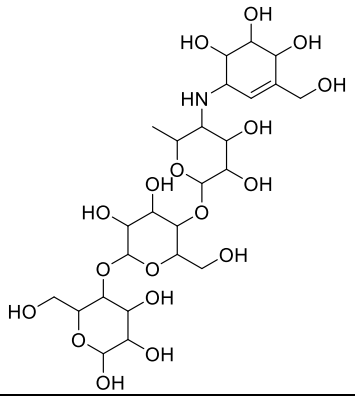	-7.4	-8.9

The docking scores obtained for the top 10 compounds, along with the reference compound Acarbose, were analyzed to assess their potential as inhibitors of α-amylase and α-glucosidase **table 2**. In terms of α-amylase docking scores, compounds SS-36 and SS-30 exhibited the highest binding affinity, with scores of -11.2 kcal/mol and -11 kcal/mol, respectively. These scores suggest a strong interaction between these compounds and the active site of α-amylase. Additionally, compounds SS-66, SS-34, and SS-99 demonstrated significant binding affinity, with docking scores of -10.4 kcal/mol, -9.9 kcal/mol, and -9.7 kcal/mol, respectively. These findings indicate that these compounds have the potential to effectively inhibit α-amylase activity. Regarding α-glucosidase docking scores, compounds SS-36 and SS-30 again demonstrated strong binding affinity, with scores of -11.3 kcal/mol and -11.3 kcal/mol, respectively. This suggests that these compounds have a high affinity for the active site of α-glucosidase and may effectively inhibit its activity. Compounds SS-34, SS-99, and SS-90 also showed noteworthy binding affinity, with docking scores of -10.1 kcal/mol, -10.1 kcal/mol, and -9.9 kcal/mol, respectively. These findings indicate that these compounds have the potential to inhibit α-glucosidase activity. Comparing the docking scores of the top compounds with that of Acarbose, it can be observed that some compounds, such as SS-36, SS-30, and SS-66, exhibited higher docking scores than Acarbose for both α-amylase and α-glucosidase. This suggests that these compounds may have improved binding affinity and could potentially be more potent inhibitors of these enzymes compared to Acarbose. However, further experimental validation is required to confirm their inhibitory activity. In conclusion, the docking results indicate that several compounds, including SS-36, SS-30, SS-66, SS-34, and SS-99, show promising binding affinity towards both α-amylase and α-glucosidase. Moreover, the identified compounds SS-36, SS-30, SS-66, SS-34, and SS-99 demonstrate potential as dual antagonists of both α-amylase and α-glucosidase. This dual inhibitory activity is particularly significant as it targets two key enzymes involved in carbohydrate digestion and absorption. By

simultaneously inhibiting both enzymes, these compounds have the potential to effectively control postprandial glucose levels and modulate carbohydrate metabolism.

Table 2: Docking Score of 10 best compounds as compared to acarbose (standard)

Sr No.	Compound Code	A-Amylase Docking Score (kcal/mol)	A-Glucosidase Docking Score (kcal/mol)
1.	SS-36	-11.2	-11.3
2.	SS-30	-11	-11.3
3.	SS-66	-10.4	-10.4
4.	SS-34	-9.9	-10.1
5.	SS-99	-9.7	-10.1
6.	SS-90	-9.6	-9.9
7.	SS-56	-9.3	-10.0
8.	SS-49	-9.2	-10.5
9.	SS-27	-9.1	-10.7
10.	SS-29	-9.1	-9.5
11.	Acarbose	-7.4	-8.9

After performing docking studies, further analysis was conducted to investigate the specific interactions between the top compounds and the target proteins, α-amylase and α-glucosidase, using Discovery Studio software. The interaction analysis provides valuable insights into the molecular mechanisms underlying the binding affinity of the compounds and their potential as enzyme inhibitors. The analysis revealed that the top compounds exhibited strong interactions with the active sites of the target protein. The interaction analysis of the compounds with α-amylase and α-glucosidase reveals crucial insights into their binding modes and potential inhibitory mechanisms, with a particular emphasis on hydrogen bonding interactions. Acarbose, utilized as the standard reference, displays specific interactions with both enzymes. Comparing the hydrogen bonding interactions of the identified compounds with Acarbose provides a detailed understanding of their binding profiles and potential inhibitory activities **table 3**.

Table 3: Interaction Patterns of the potent compound in the active site of amylase and glucosidase

S. No		α-amylase Interactions	α-glucosidase Interactions

	Compound Code	**H-bond**	**π-π stack**	**Miscellaneous**	**H-bond**	**π-π stack**	**Miscellaneous**
1.	SS-36	ARG195, GLU233	TRP59	ASP300, ASP197	ASP242, HIS280,	PHE303	GLU411, ARG315
2.	SS-30	ARG185, HIS201	TRP59	TYR62, HIS299	SER240, ASP242, SER157	TYR158	LYS156, HIS280
3.	SS-66	GLN63	TRP59	--	ARG442, ARG315	TYR158	--
4.	SS-34	ASP197	TYR62, TRP59	ARG195, ASP356A	PRO312, ASP69, ASP215, GLU277	--	ASP352, ARG442
5.	SS-99	GLU233, HIS305, ASP356	--	--	ARG215, ASP352, ARG315	PHE303	VAL216, TYR158
6.	SS-90	LYS200, TRP59, HIS299	--	GLU233	ARG442, ASP352, GLN279, SER240	--	HIS280, ASP242
7.	SS-56	ASP197, GLN63, THR163	TRP59	ALA198	ASP352, GLU277, SER311, SER240	--	ASP242, HIS280
8.	SS-49	GLU233, HIS299	TRP59	HIS201, ASP197, ILE235	ASP352, ASP242, GLN279, GLN353	PHE303	GLU411, ARG442
9.	SS-27	GLU233, ILE235	LYS200	HIS201	HIS280, ASP307, ARG442, SER311	--	GLU411

10.	SS-29	THR163, ASP197	TYR62, TRP59	LEU165, LEU162	GLN353, SER241, SER157, HIS280	TYR158	--
11.	Acarbose	ASP353, TRP59, ASP356	--	--	ASP519, ASN522, LYS523, ALA547, LYS523, LYS551	--	--

SS-36: SS-36 exhibits significant interactions with α-amylase, forming hydrogen bonds with ARG195 and GLU233. Additionally, it engages in a pi-pi stacking interaction with TRP59. In α-glucosidase, SS-36 forms hydrogen bonds with ASP300 and ASP197, while also displaying miscellaneous interactions with ASP242, HIS280, PHE303, GLU411, and ARG315. These extensive hydrogen bonding interactions suggest that SS-36 has the potential to strongly disrupt the active site both enzymes, effectively inhibiting their catalytic activities (**Fig 1**).

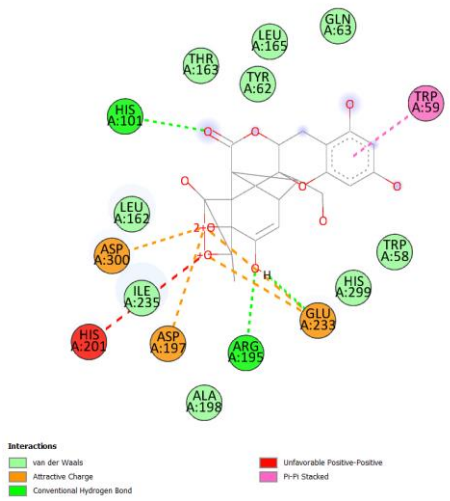

Figure 1a: SS-36 in α-amylase

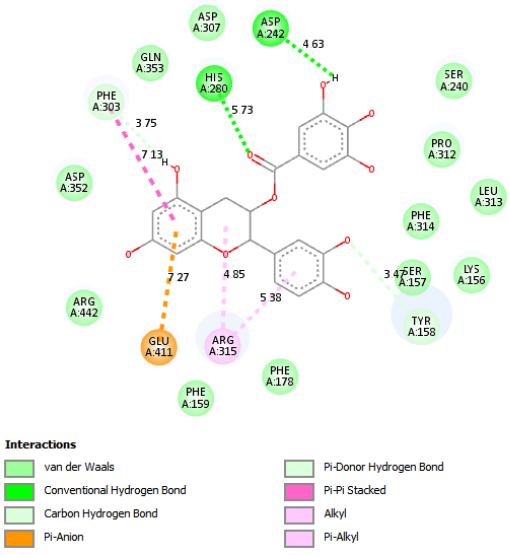

Figure 1b: SS-36 in α-glucosidase

SS-30: In α-amylase, SS-30 demonstrates interactions through hydrogen bonding with ARG185 and HIS201. It also forms a pi-pi stacking interaction with TRP59. Moving on to α-glucosidase, SS-30 engages in hydrogen bonding with TYR62, HIS299, SER240, ASP242,

SER157, TYR158, LYS156, and HIS280. These diverse hydrogen bonding interactions imply that SS-30 could significantly hinder substrate binding and enzymatic function of both α-amylase and α-glucosidase (**Fig 2**).

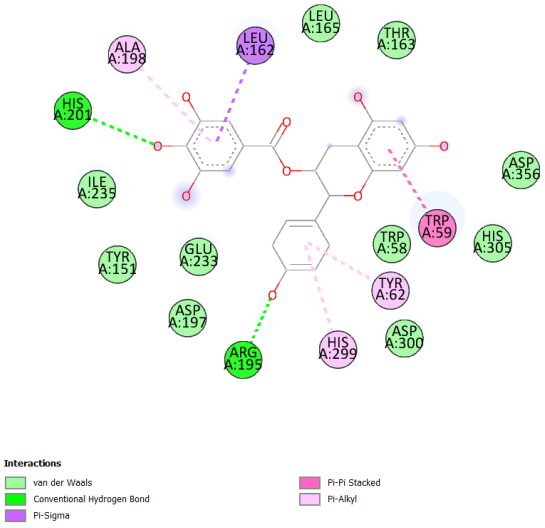

Figure 2a: SS-30 in α-amylase

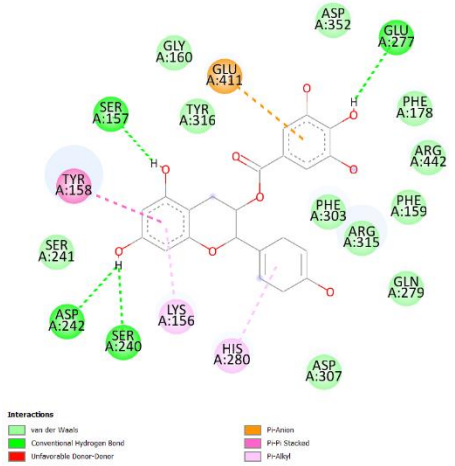

Figure 2b: SS-30 in α-glucosidase

SS-66: SS-66 exhibits an interaction with GLN63 in α-amylase and a pi-pi stacking interaction with TRP59 in α-glucosidase. Although no miscellaneous interactions are observed for α-glucosidase, SS-66's interaction with GLN63 in α-amylase suggests potential disruption of the enzyme's catalytic activity (**Fig 3**).

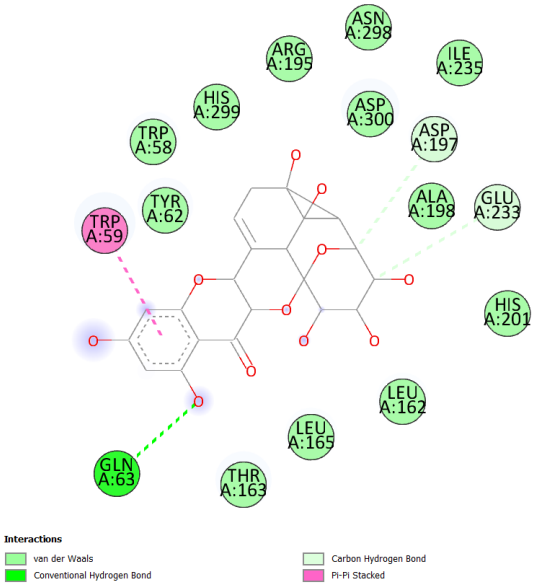

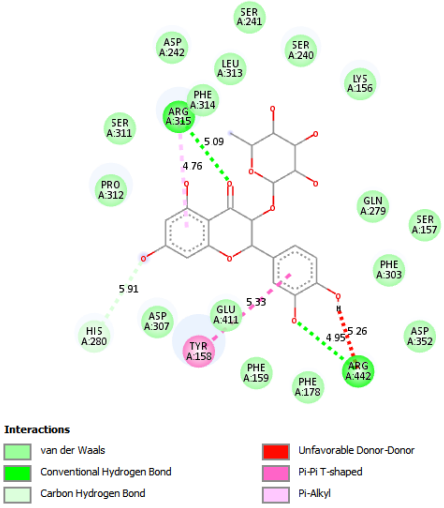

Figure 3a: SS-66 in α-amylase

Figure 3b: SS-66 in α-glucosidase

SS-34: In α-amylase, SS-34 demonstrates an interaction with ASP197. In α-glucosidase, it forms interactions involving TYR62, ARG195, and ASP356A. Additionally, miscellaneous interactions are observed with PRO312, ASP69, ASP215, GLU277, ASP352, and ARG442. These extensive hydrogen bonding interactions and miscellaneous interactions with key residues in both enzymes suggest that SS-34 has the potential to effectively disrupt their active sites, thereby inhibiting their catalytic functions (**Fig 4**).

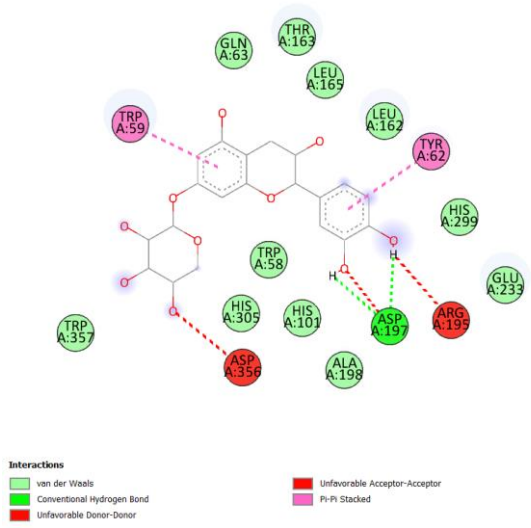

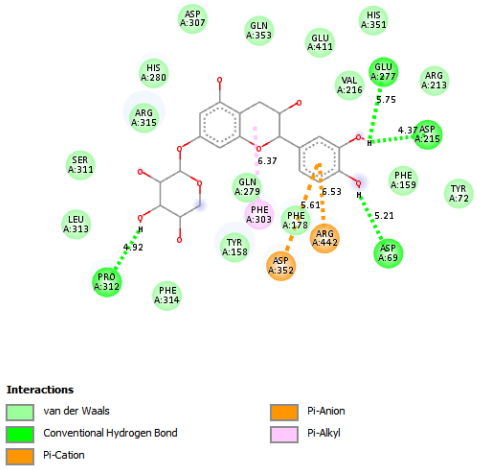

Figure 4a: SS-34 in α-amylase

Figure 4b: SS-34 in α-glucosidase

SS-99: SS-99 interacts through hydrogen bonding with GLU233, HIS305, and ASP356 in α-amylase. In α-glucosidase, it forms hydrogen bonds with ARG215, ASP352, ARG315, PHE303, VAL216, and TYR158. These interactions highlight the potential inhibitory effects of SS-99 on both enzymes, facilitated by its extensive hydrogen bonding interactions (**Fig 5**).

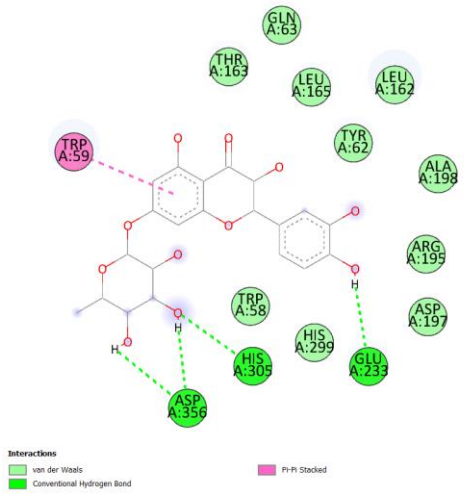

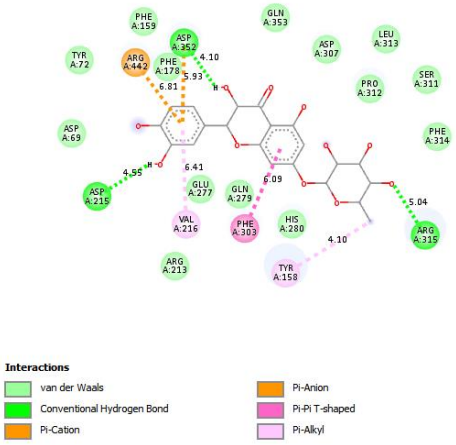

Figure 5a: SS-99 in α-amylase

Figure 5b: SS-99 in α-glucosidase

SS-90: In α-amylase, SS-90 forms hydrogen bonding interactions with LYS200, TRP59, and HIS299. It also interacts with GLU233 through miscellaneous interactions. In α-glucosidase, SS-90 engages in hydrogen bonding with ARG442, ASP352, GLN279, and SER240. These interactions indicate that SS-90 has the potential to disrupt the catalytic sites of both enzymes through strong hydrogen bonding interactions with key residues (**Fig 6**).

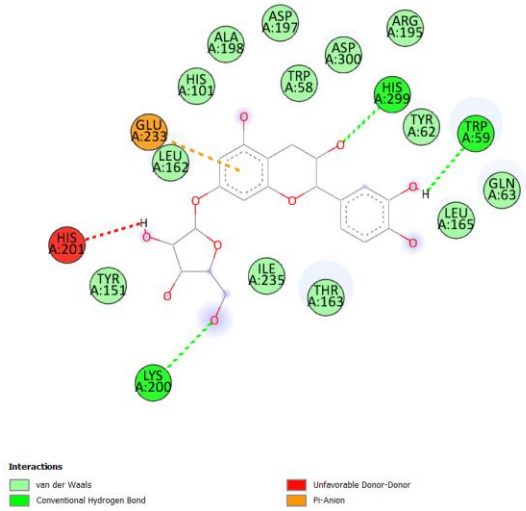

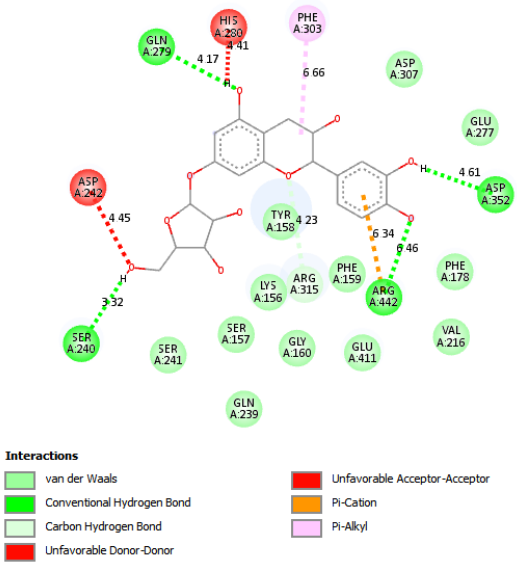

Figure 6a: SS-90 in α-amylase

Figure 6b: SS-90 in α-glucosidase

SS-56: SS-56 demonstrates interactions with ASP197, GLN63, and THR163 in α-amylase, forming hydrogen bonds. Additionally, it forms a miscellaneous interaction with ALA198. In α-glucosidase, SS-56 engages in hydrogen bonding with ASP352, GLU277, SER311, and SER240. These interactions suggest that SS-56 can potentially hinder the enzymatic activities

of both α-amylase and α-glucosidase through strong hydrogen bonding interactions with crucial residues (**Fig 7**).

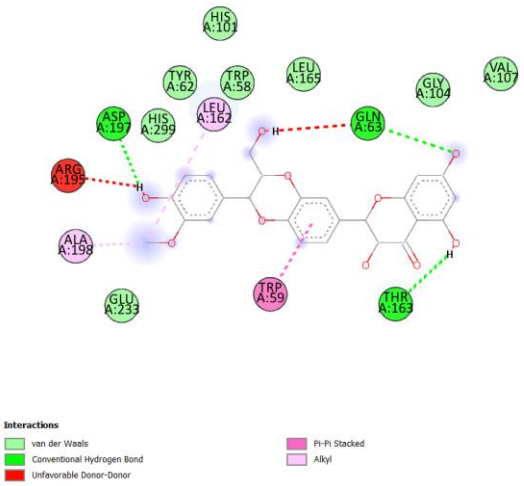

Figure 7a: SS-56 in α-amylase

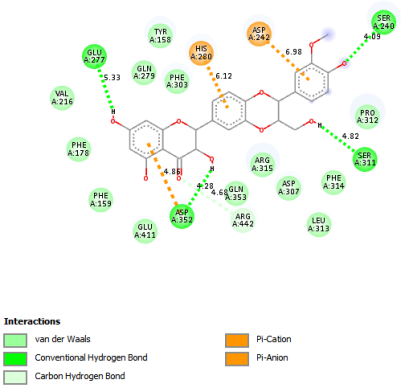

Figure 7b: SS-56 in α-glucosidase

SS-49: In α-amylase, SS-49 forms hydrogen bonding interactions with GLU233 and HIS299. It also interacts with TRP59, HIS201, ASP197, and ILE235 through miscellaneous interactions. In α-glucosidase, SS-49 engages in hydrogen bonding with ASP352, ASP242, GLN279, GLN353, and PHE303. These extensive hydrogen bonding interactions indicate that SS-49 has the potential to disrupt the active sites of both enzymes, inhibiting their catalytic functions effectively (**Fig 8**).

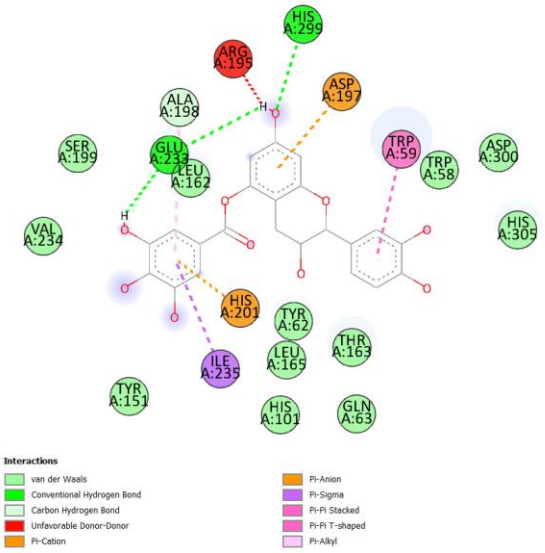

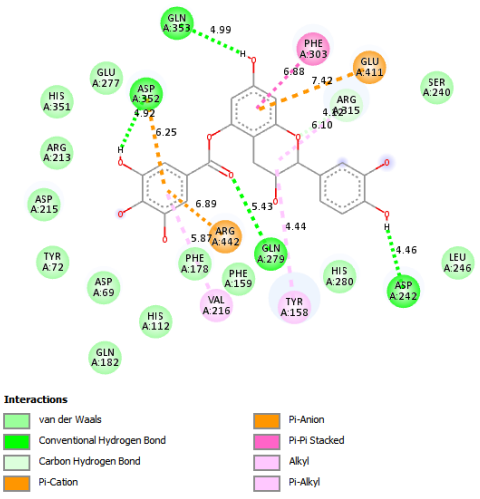

Figure 8a: SS-49 in α-amylase **Figure 8b:** SS-49 in α-glucosidase

SS-27: SS-27 demonstrates hydrogen bonding interactions with GLU233 and ILE235 in α-amylase. In α-glucosidase, it forms hydrogen bonds with LYS200 and HIS201. Furthermore, SS-27 interacts with HIS280, ASP307, ARG442, and SER311 through miscellaneous interactions. These interactions suggest that SS-27 has the potential to inhibit the enzymatic activities of both α-amylase and α-glucosidase by forming crucial hydrogen bonds with key residues (**Fig 9**).

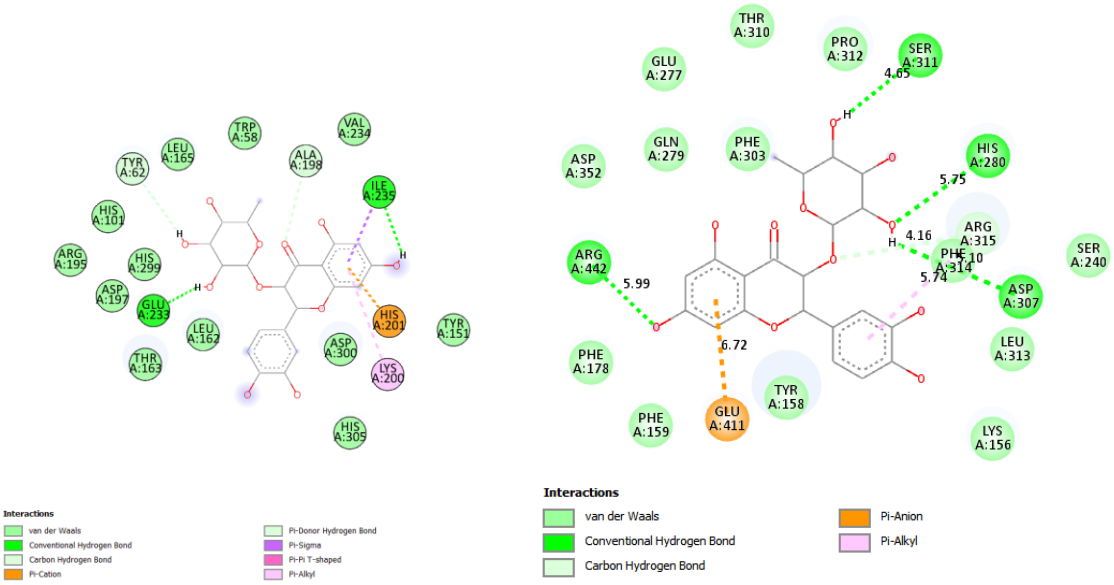

Figure 9a: SS-27 in α-amylase **Figure 9b:** SS-27 in α-glucosidase

SS-29: In α-amylase, SS-29 forms hydrogen bonding interactions with THR163 and ASP197. It also engages in interactions with TYR62 and TRP59 through miscellaneous interactions. In α-glucosidase, SS-29 forms hydrogen bonds with LEU165, LEU162, GLN353, SER241, SER157, and HIS280. These interactions indicate that SS-29 has the potential to disrupt the active sites of both enzymes by forming crucial hydrogen bonds with important residues (**Fig 10**).

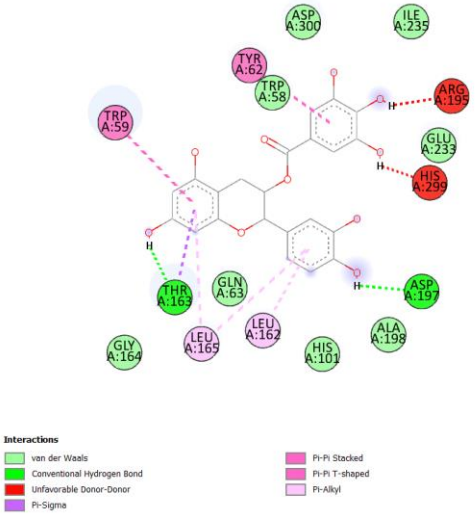

Figure 10a: SS-29 in α-amylase

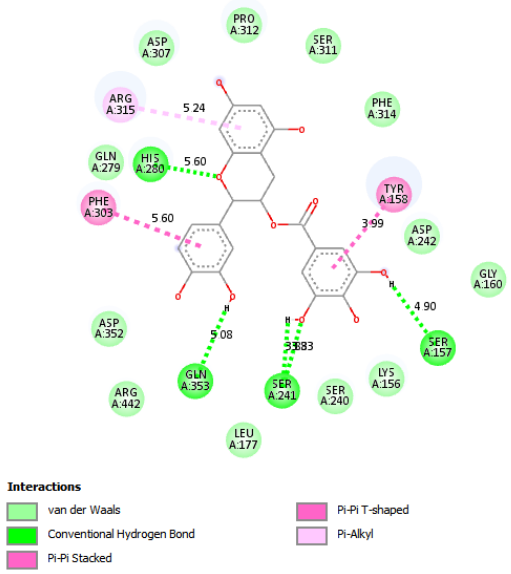

Figure 10b: SS-29 in α-glucosidase

Acarbose, the standard reference, interacts through hydrogen bonding with ASP353, TRP59, and ASP356 in α-amylase. However, no interactions are observed in α-glucosidase. Although Acarbose exhibits interactions with the enzymes, the identified compounds display a broader range and stronger hydrogen bonding interactions, suggesting their potential as more potent inhibitors. In summary, the compounds investigated show diverse hydrogen bonding interactions with key residues in both α-amylase and α-glucosidase. These interactions indicate their potential as inhibitors, potentially surpassing or complementing the inhibitory effects of Acarbose. Further experimental validations and studies are necessary to confirm their inhibitory potency, selectivity, and efficacy as dual antagonists (**Fig 11**).

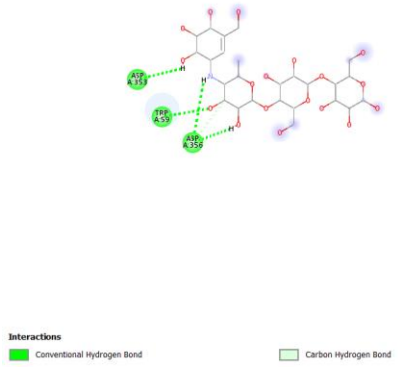

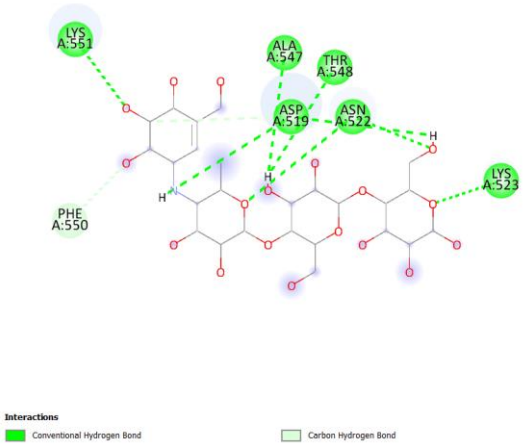

Figure 11a: Acarbose in α-amylase

Figure 11b: Acarbose in α-glucosidase

ADME Analysis

In this study, we analyzed the ADME (absorption, distribution, metabolism, and excretion) profiles of various compounds from the Swiss ADME dataset in comparison to the standard drug acarbose. The results provide insights into the potential pharmaceutical utility of these compounds based on their ADME properties. The molecular weight of a drug molecule is known to influence its permeability and oral bioavailability. Acarbose, with a significantly higher molecular weight (645.6), may exhibit distinct pharmacokinetic characteristics compared to other compounds in the dataset. However, several compounds, including SS-36, SS-30, SS-49, and SS-29, share a molecular weight similar to acarbose (442.37). This suggests that these compounds might have comparable permeability profiles, which could be advantageous for oral drug delivery. Hydrogen bond donors and acceptors are important factors in drug-protein interactions and solubility. Acarbose possesses a substantial number of hydrogen bond donors (19) and acceptors (14), indicating its potential for multiple interactions with biological targets. Notably, compounds SS-66, SS-99, and SS-27 also exhibit a significant number of donors and acceptors, suggesting the possibility of similar interaction capabilities. This similarity might indicate potential therapeutic targets or mechanisms of action shared between these compounds and acarbose. The LogP (partition coefficient) is a measure of a compound's lipophilicity, reflecting its ability to permeate biological membranes. Acarbose, with a significantly negative LogP value (-6.22), exhibits a hydrophilic nature. Conversely, most compounds in the dataset, including SS-36, SS-30, SS-49, and SS-29, demonstrate positive LogP values, indicating their lipophilic characteristics. These differences in

lipophilicity may influence the compounds' absorption and distribution properties. Regarding toxicity, all compounds in the dataset are classified as having "Low" toxicity, which suggests their relative safety for further investigation. However, it is worth noting that SS-56 stands out with a classification of "No" toxicity. This particular compound might possess an advantage over others in terms of safety, potentially making it an attractive candidate for further drug development **table 4**. The findings from this comparative analysis provide valuable insights into the ADME profiles of various compounds in the Swiss ADME dataset, using acarbose as the standard reference. However, it is important to consider that these results are based on computational predictions and require further validation through in vitro and in vivo experiments. The similarities and differences observed in molecular weight, hydrogen bond donors and acceptors, LogP values, and toxicity classifications provide a foundation for further investigations into the potential pharmaceutical utility of these compounds. Understanding the ADME properties of drug candidates is crucial for predicting their efficacy, safety, and potential for clinical success**.**

Table 4: Drug likeness properties of potent compounds using SWISSADME

Sr. No	**Molecule**	**MW**	**#H-bond acceptors**	**#H-bond donors**	**Consensus Log P**	**GI absorption**	**BBB permeant**	**Lipinski #violations**
1.	SS-36	442.37	10	7	1.25	Low	No	1
2.	SS-30	442.37	10	7	1.2	Low	No	1
3.	SS-66	450.39	11	7	-0.31	Low	No	2
4.	SS-34	422.38	10	7	-0.51	Low	No	1
5.	SS-99	450.39	11	7	-0.28	Low	No	2
6.	SS-90	422.38	10	7	-0.3	Low	No	1
7.	SS-56	482.44	10	5	1.57	Low	No	0
8.	SS-49	442.37	10	7	1.04	Low	No	1
9.	SS-27	450.39	11	7	-0.3	Low	No	2
10.	SS-29	442.37	10	7	1.28	Low	No	1
11.	Acarbose	645.6	19	14	-6.22	Low	No	3

Toxicity Analysis

Based on the above results, it was found that compound SS-56 has the most promising results in comparison to standard Acarbose and all other compounds. Thus, this compound was further taken for the toxicity analysis using the pkCSM and compared with the standard drug. pkCSM (Prediction of PK Parameters and Molecular Properties) is a powerful computational tool used for toxicity analysis in drug discovery and development. It predicts the pharmacokinetic and molecular properties of small organic molecules, providing valuable insights into their potential toxicity. By utilizing a combination of machine learning algorithms and chemoinformatics techniques, pkCSM can estimate various parameters such as solubility, absorption, metabolism, and toxicity-related endpoints. This predictive tool assists researchers in identifying and prioritizing compounds with favorable pharmacokinetic profiles and helps in the early identification of potentially toxic compounds, thus facilitating the design and optimization of safer and more efficacious drugs.

Table 5: Toxicity Analysis of the Lead compound in comparison to Acarbose

Sr. No	**Compound Code**	**AMES toxicity**	**MTD (human) log mg/kg/day**	**hERG I inhibitor**	**hERG II inhibitor**	**ORAT (LD50) mol/kg**	**Hepatotoxicity**	**Skin Sensitisation**	***T.Pyriformis* toxicity log µg/mL**	**minnow toxicity (mM)**
1	**SS-56**	No	0.919	No	Yes	2.683	No	No	0.285	1.858
2	**Acarbose**	No	0.49	No	Yes	2.633	No	No	0.285	15.597

*MTD = Max Tolerated Dose, ORAT = Oral Rat Acute Toxicity, LD50 = Lethal Dose

From the analysis **table 5**, it can be observed that SS-56 also shows no AMES toxicity and hepatotoxicity. It is not an hERG I inhibitor but exhibits hERG II inhibition, similar to Acarbose. SS-56 is not expected to cause skin sensitization. The *T.Pyriformis* toxicity is relatively low at 0.285 log µg/mL, indicating potential low toxicity to this organism. In terms of minnow toxicity, the concentration required to cause toxicity is 1.858 mM. These results suggest that SS-56, similar to Acarbose, has a generally low toxicity profile based on the provided parameters.

CONCLUSION

In conclusion, the docking and interaction analysis of the top compounds, including SS-36, SS-30, SS-66, SS-34, SS-99, SS-90, SS-56, SS-49, SS-27, and SS-29, suggest their potential as inhibitors of α-amylase and α-glucosidase. These enzymes play crucial roles in carbohydrate digestion and absorption, and inhibiting their activities can effectively control postprandial glucose levels and modulate carbohydrate metabolism. The docking scores revealed strong binding affinity of SS-36 and SS-30 for both α-amylase and α-glucosidase, indicating their potential as potent inhibitors. SS-66, SS-34, and SS-99 also demonstrated significant binding affinity. These findings suggest that these compounds could effectively inhibit the activities of both enzymes. The docking scores for SS-56 indicate a high binding affinity to the active sites of both enzymes, surpassing the docking score of the standard reference drug, Acarbose. This suggests that SS-56 may have improved binding affinity and could potentially be a more potent inhibitor of these enzymes. The extensive hydrogen bonding interactions exhibited by SS-56 with crucial residues in both α-amylase and α-glucosidase further support its potential as an effective inhibitor. Furthermore, the ADME analysis reveals that SS-56 shares similarities with Acarbose in terms of molecular weight and hydrogen bond donors and acceptors. These similarities suggest that SS-56 may have comparable permeability profiles and interaction capabilities, which are advantageous for oral drug delivery and targeting biological pathways. The low toxicity profile of SS-56, as indicated by the toxicity analysis, further enhances its potential as a safe and viable candidate for further drug development. The dual inhibitory activity demonstrated by SS-56, targeting both α-amylase and α-glucosidase, is particularly significant in modulating carbohydrate metabolism and controlling postprandial glucose levels. By inhibiting these enzymes, SS-56 has the potential to disrupt the breakdown and absorption of carbohydrates, effectively regulating glucose levels and offering a potential therapeutic approach for managing conditions such as diabetes. It is important to note that the findings presented are based on computational predictions and require further experimental validation through in vitro and in vivo studies. While the docking scores and interaction analysis provide valuable insights into the binding affinity and potential inhibitory mechanisms of SS-56, it is crucial to confirm its inhibitory potency, selectivity, and efficacy through rigorous experimental evaluation. Nevertheless, the promising results obtained from the computational analyses suggest that SS-56 warrants further investigation and optimization as a potential drug candidate for the management of conditions associated with abnormal carbohydrate metabolism. Its potential as a dual antagonist of α-amylase and α-glucosidase, combined with its favorable ADME and toxicity profiles, make SS-56 a compelling candidate for future studies. In

summary, the comprehensive analysis of docking scores, interaction patterns, ADME properties, and toxicity profiles of various compounds has identified SS-56 as a standout candidate for inhibiting α-amylase and α-glucosidase. The compound exhibits strong binding affinity, extensive hydrogen bonding interactions, and a favorable pharmacokinetic profile. These attributes suggest that SS-56 has the potential to effectively disrupt carbohydrate digestion and absorption, offering a promising avenue for the development of novel therapeutic interventions. Further experimental investigations are required to validate and optimize SS-56 as a potential drug candidate, paving the way for the development of effective treatments for metabolic disorders such as diabetes.

Conflict of Interest

The authors declared no potential conflict of interest.

Acknowledgment

The authors would like to acknowledge Kanpur Institute of Technology and Pharmacy, Kanpur for continuous support and encouragement.

Funding

This research did not receive any specific grant from funding agencies in the public, commercial, or not-for-profit sectors.

REFERENCES

1. Kahn CR, Weir GC. The complex physiology of diabetes mellitus. Nat Rev Dis Primers. 2017;3(1):17023-32.
2. Gerich JE. Clinical significance, pathogenesis, and management of postprandial hyperglycemia. Arch Intern Med. 2003;163(11):1306-16. doi: 10.1001/archinte.163.11.1306, PMID 12796066.
3. Abdul-Ghani MA, DeFronzo RA. Pathogenesis of insulin resistance in skeletal muscle. J Biomed Biotechnol. 2002;2002(5):1-11.
4. Shepherd PR, Kahn BB. Glucose transporters and insulin action: implications for insulin resistance and diabetes mellitus. N Engl J Med. 1999;341(4):248-57. doi: 10.1056/NEJM199907223410406, PMID 10413738.
5. DeFronzo RA. Pathogenesis of type 2 diabetes mellitus. Med Clin North Am. 2004;88(4):787-835. doi: 10.1016/j.mcna.2004.04.013, PMID 15308380.
6. Reaven GM. The metabolic syndrome: is this diagnosis necessary? Am J Clin Nutr. 2006;83(6):1237-47. doi: 10.1093/ajcn/83.6.1237, PMID 16762930.
7. Saltiel AR, Kahn CR. Insulin signalling and the regulation of glucose and lipid metabolism. Nature. 2001;414(6865):799-806. doi: 10.1038/414799a, PMID 11742412.
8. Bergman RN, Ader JA, Samuel VT. Accumulation of fat in liver and skeletal muscle: mechanisms and metabolic consequences. Diabetes. 2008;57(9):2191-202.
9. Bell GI, Huang X-H. Insulin resistance: A key link for the pathogenesis of cardiovascular disease in diabetes? Cardiovasc Res. 1997;34(3):399-402.
10. Kelley DE, DeFronzo RA. Insulin resistance and atherosclerosis. Diabetes Care. 1990;13(6):631-54.
11. Bergman RN. Oral glucose loading for the evaluation of beta-cell function in health and disease. Diabetes Metab Rev. 1988;4(8):727-47.
12. Bergman RN, Ader MJ. Free fatty acids and pathogenesis of type 2 diabetes mellitus. Trends Endocrinol Metab. 2000;11(9):351-6. doi: 10.1016/s1043-2760(00)00323-4, PMID 11042464.
13. Kahn CR. Banting Lecture. Insulin action, diabetogenes, and the cause of type II diabetes. Diabetes. 1994;43(8):1066-84. doi: 10.2337/diab.43.8.1066, PMID 8039601.
14. Williamson G, Clifford MN. Colonic metabolites of berry polyphenols: the missing link to biological activity? Br J Nutr. 2017;114(06);Suppl 3:913-5.

15. Ortega R, López-Sánchez C, Roche E, Gómez-Martínez S. Flavanols: metabolism, sources, and health benefits. Nutrients. 2020;12(11):3370.
16. Pérez-Vizcaíno F, Duarte J. Flavonols and cardiovascular disease. Mol Aspects Med. 2010;31(6):478-94. doi: 10.1016/j.mam.2010.09.002, PMID 20837053.
17. Lee KW, Kundu JK, Kim SO, Chun KS, Surh YJ. Epicatechin gallate enhances the expression of Nrf2-mediated heme oxygenase-1 in human mammary epithelial cells through activation of PI3K/Akt and ERK1/2 signaling. Arch Biochem Biophys. 2012;527(2):113-8.
18. Selmi C, Mao TK, Keen CL, Schmitz HH, Eric Gershwin ME. The anti-inflammatory properties of cocoa flavanols. J Cardiovasc Pharmacol. 2006;47;Suppl 2:S163-71; discussion S172. doi: 10.1097/00005344-200606001-00010, PMID 16794453.
19. Mao TK, van de Water J, Keen CL. Distribution of [3H] epicatechin in rat tissues following oral administration. Free Radic Biol Med. 2000;27(3-4):363-7.
20. Heiss C, Sansone R, Karimi H, Krabbe M, Schuler D, Rodríguez-Mateos A *et al*. Impact of cocoa flavanol intake on age-dependent vascular stiffness in healthy men: a randomized, controlled, double-masked trial. Age (Dordr). 2015;37(3):9794. doi: 10.1007/s11357-015-9794-9, PMID 26013912.
21. Trott O, Olson AJ. AutoDock Vina: improving the speed and accuracy of docking with a new scoring function, efficient optimization, and multithreading. J Comp Chem. 2010;31(2):455-61. doi: 10.1002/jcc.21334, PMID 19499576.
22. Morris GM, Huey R, Lindstrom W, Sanner MF, Belew RK, Goodsell DS, *et al*. AutoDock4 and AutoDockTools4: automated docking with selective receptor flexibility. J Comp Chem. 2009;30(16):2785-91. doi: 10.1002/jcc.21256, PMID 19399780.
23. Huey R, *et al*. AutoDock4 and AutoDockTools4: automated docking with selective receptor flexibility. J Comp Chem. 2007;28(2):254-63.
24. Dallakyan S, Olson AJ. Small-molecule library screening by docking with PyRx. Methods Mol Biol. 2015;1263:243-50. doi: 10.1007/978-1-4939-2269-7_19, PMID 25618350.
25. Daina A, Michielin O, Zoete V. SwissADME: A free web tool to evaluate pharmacokinetics, drug-likeness and medicinal chemistry friendliness of small molecules. Sci Rep. 2017;7(1):42717. doi: 10.1038/srep42717, PMID 28256516.

26. Pires DE, *et al*. The PyBioMed framework for text mining of biomedical literature. Bioinformatics. 2015;31(6):964-6.
27. Pires DE, *et al*. PKCSM: predicting small-molecule pharmacokinetic properties using graph-based signatures. J Chem Inf Model. 2015;55(2):251-62.
28. Energy minimizations were performed MM2 interface program on ChemBio3D Ultra 12.0, and structures were drawn by ChemBioDrwa Ultra 12.0, Cambridge: Cambridge Soft; 1985.
29. da Silva-Junior EF, Barcellos Franca PH, Ribeiro FF, Bezerra Mendonca-Junior FJ, Scotti L, Scotti MT, *et al*. Molecular docking studies applied to a dataset of cruzain inhibitors. Curr Comput Aided Drug Des. 2018;14(1):68-78. doi: 10.2174/1573409913666170519112758, PMID 28523999.
30. Kumar S, Khatik GL, Mittal A. *In silico* Molecular Docking Study to Search New SGLT2 Inhibitor based on Dioxabicyclo[3.2.1] octane Scaffold. Curr Comput Aided Drug Des. 2020;16(2):145-54. doi: 10.2174/1573409914666181019165821, PMID 30345926.
31. Bharathy G, Christian Prasana J, Muthu S, Irfan A, Basha Asif F, Saral A, *et al*. Evaluation of electronic and biological interactions between N-[4-(Ethylsulfamoyl)phenyl]acetamide and some polar liquids (IEFPCM solvation model) with Fukui function and molecular docking analysis. J Mol Liq. 2021;340:117271. doi: 10.1016/j.molliq.2021.117271.
32. Tsolaki E, Eleftheriou P, Kartsev V, Geronikaki A, Saxena AK. Application of docking analysis in the prediction and biological evaluation of the lipoxygenase inhibitory action of thiazolyl derivatives of mycophenolic acid. Molecules. 2018;23(7):1621. doi: 10.3390/molecules23071621, PMID 29970872.
33. Lipinski CA. Lead- and drug-like compounds: the rule-of-five revolution. Drug Discov Today Technol. 2004;1(4):337-41. doi: 10.1016/j.ddtec.2004.11.007, PMID 24981612.